ELSEVIER

Journal of Power Sources 111 (2002) 176–180

JOURNAL OF POWER SOURCES

www.elsevier.com/locate/jpowsour

Short communication

Electrochemical properties of iodine-containing lithium manganese oxide spinel

Chi-Hwan Han, Young-Sik Hong, Hyun-Sil Hong, Keon Kim*

Research Division of Chemistry and Molecular Engineering, Department of Chemistry, Korea University, Seoul 136-701, South Korea

Received 21 December 2001; accepted 19 February 2002

Abstract

Iodine-containing, cation-deficient, lithium manganese oxides (ICCD-LMO) are prepared by reaction of MnO_2 with LiI. The MnO_2 is completely transformed into spinel-structured compounds with a nominal composition of $Li_{1-\delta}Mn_{2-2\delta}O_4I_x$. A sample prepared at 800 °C, viz. $Li_{0.99}Mn_{1.98}O_4I_{0.02}$, exhibits an initial discharge capacity of 113 mA h g^{-1} with good cycleability and rate capability in the 4-V region. Iodine-containing, lithium-rich lithium manganese oxides (ICLR-LMO) are also prepared by reaction of $LiMn_2O_4$ with LiI, which results in a nominal composition of $Li_{1+x}Mn_{2-x}O_4I_x$. $Li_{1.01}Mn_{1.99}O_4I_{0.02}$ shows a discharge capacity of 124 mA h g^{-1} on the first cycle and 119 mA h g^{-1} a on the 20th cycle. Both results indicate that a small amount of iodine species helps to maintain cycle performance.

Keywords: Lithium-ion battery; Iodine-containing; Lithium manganese oxide

1. Introduction

Spinel-structured lithium manganese oxides (LMO) have been widely investigated as a cathode materials for compact, high-voltage, rechargeable lithium-ion batteries. Although $LiCoO_2$ and $LiNiO_2$ are in advanced stages of development and commercialization, they have economic and environmental disadvantages that leave the door open to exploit alternative cathode materials. In this respect, LMO attracts interest because of its low cost and good safety. The substitution of LMO for $LiCoO_2$ has not been successful, however, due to the capacity degradation of LMO during charge–discharge cycling [1,2].

From a structural viewpoint, spinel LMO with Li:Mn = 0.5 can be classified into two major groups [3]. One is cation-deficient $Li_{1-\delta}Mn_{2-2\delta}O_4$, the other is lithium-rich $Li_{1+x}Mn_{2-x}O_4$. In these compounds, a decrease in theoretical capacity cannot be avoided for the sake of good cycle performance. In attempts to improve cycleability, several studies have been directed to anion-substituted compounds. Amatucci et al. [4] have shown that the storage performance at elevated temperature is improved in fluoride-substituted LMO, as well as capacity and its retention [4]. Similarly, sulfide-substituted LMO and amorphous manganese oxyiodide have been investigated [5,6]. Along with these intrinsic factors, the extrinsic factors coming from the synthesis conditions, such as oxygen partial pressure and reaction temperature, have been studied [7–11].

In this investigation, we have prepared two series of iodine-containing, cation-deficient $Li_{1-\delta}Mn_{2-2\delta}O_4I_x$ (ICCD-LMO) and lithium-rich $Li_{1+x}Mn_{2-x}O_4I_x$ (ICLR-LMO), to examine the role of iodine species.

2. Experimental

Powders of ICCD-LMO were prepared from direct reaction of LiI/MnO_2 = 1/2 at temperature ranges of 500–900 °C for 12 h in air. The heating rate was set at 200 °C h^{-1} for all temperature settings. To prepare ICLR-LMO, stoichiometric $LiMn_2O_4$ was prepared by intimately mixing Li_2CO_3 and MnO_2 in the ratio 1:4, followed by heating at 850 °C for 24 h in air. Subsequently, $LiMn_2O_4$ was reacted with LiI at 400 °C for 4 h, according to the nominal compositions (x = 0.02, 0.04, 0.07, 0.10).

The cation composition of the products was determined by inductively coupled plasma (ICP) spectroscopy after dissolving the powders in dilute nitric acid. The amount of iodine species was determined by gravimetry, as follows. The dissolved samples were reacted with excess silver nitrate solution and then aged for 2 days at 5 °C. The

* Corresponding author.
E-mail address: kkim@mail.korea.ac.kr (K. Kim).

0378-7753/02/$ – see front matter
PII: S0378-7753(02)00098-8

resulting yellowish precipitate was filtered and weighed. The oxygen content was determined from the mass balance. The morphology and microstructure of the powders were examined by means of field emission scanning electron microscopy (FE-SEM, Hitachi S-4300). The crystal structure was analyzed by X-ray diffraction (XRD) using a MAC Science MXP3A-HF diffractometer and, the Rietveld method with the Fullprof Program [12]. The scanned data were collected in the 2θ range of 15–100°. The step size was 0.026° with counting time of 3 s.

The electrochemical characteristics were studied using a two-electrode cell. The working electrode, which consisted of 16 mg of cathode active material (80 wt.%), 3 mg of acetylene black (15 wt.%) and 1 mg of PTFE (5 wt.%), was pressed and then vacuum dried at 120 °C for 24 h. Lithium metal and polypropylene film were used as a counter electrode and a separator, respectively. The electrolyte was 1 M $LiPF_6$ in 1:1 ethylene carbonate/dimethyl carbonate solution. The cells were tested at a constant current of 70 or 280 mA g^{-1} in the voltage range 4.5–3.5 V with an Arbin charge–discharge cycler (BT 2042). After 20 cycles, XRD was performed on a composite cathode pellet ex situ at the end of discharge. Cyclic voltammetry (CV) was performed at a scan rate of 50 μV s^{-1} by means of a Zahner AC Impedance Analyzer (IM6).

3. Results and discussion

3.1. Chemical analysis

According to the chemical analysis, it is worthy to note that ICCD- and ICLR-LMO series contain a significant amount of iodine species even though the iodine content decreases with increasing reaction temperature (as shown in Table 1). The existence of iodine species could be clearly identified by the yellow colour in the dissolved solution. According to Kim and Manthiram [13], the content of iodine species in amorphous manganese oxyiodide decreases as the firing temperature increases, and completely disappears above the synthesis temperature of 600 °C. Consequently, it can be concluded that the iodine species in ICCD-LMO is more durable to higher temperature than those in amorphous manganese oxyiodide.

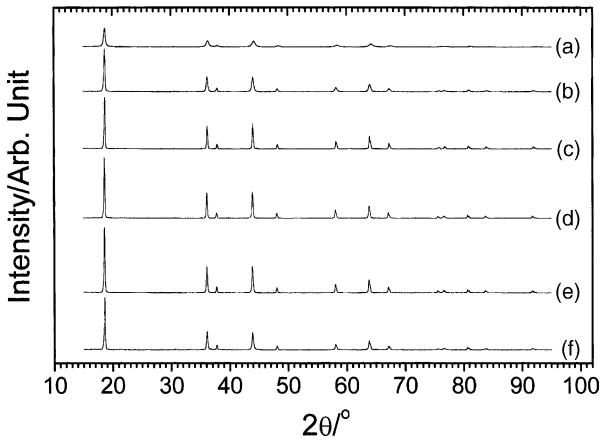

Fig. 1. Powder XRD patterns of ICCD-LMO prepared at: (a) 500 °C, (b) 800 °C, and (c) 900 °C; ICLR-LMO with: (d) $x = 0$, (e) $x = 0.02$, and (f) $x = 0.07$.

3.2. Structural analysis (XRD and FT-IR)

The XRD patterns of ICCD- and ICLR-LMO are presented in Fig. 1 and a single-phase spinel structure with the space group *Fd3m*. Because it is difficult to confirm the site and occupancy of lithium ions, the occupancies of lithium in 8a sites and manganese ions in 16d sites are fixed according to the spinel composition $LiMn_2O_4$ and the iodine species are not included. Then, the refinement gives good agreement factors of, for instance $R_p = 10.2\%$, $R_{wp} = 12.9\%$, and $R_I = 2.59\%$ for ICCD-LMO prepared at 800 °C. The lattice parameters of ICCD-LMO increase with decrease of manganese valence as the reaction temperature increases (Table 1). Similarly, the lattice parameters of ICLR-LMO decrease with increasing x. It is well-known that the lattice parameter a decreases with the increase in excess lithium occupying 16d sites, because of the increase of manganese valence.

3.3. Morphological analysis (FE-SEM)

FE-SEM of ICCD- and ICLR-LMO powders are shown in Fig. 2. It should be noted that the morphologies of ICCD-LMO prepared in the temperature range 500–800 °C are quite different from that of ICCD-LMO prepared at 900 °C.

Table 1
Lattice parameters and chemical analysis of ICCD- and ICLR-LMOs

ICCD-LMO				ICLR-LMO			
Temperature (°C)	a (Å)	Composition	Mn valency	x	a (Å)	Composition	Mn valency
500	8.197 (2)	$Li_{0.98}Mn_{1.97}O_4I_{0.11}$	3.62	0	8.243 (2)	$Li_{0.99}Mn_{2.00}O_4$	3.51
600	8.210 (5)	$Li_{0.98}Mn_{1.98}O_4I_{0.06}$	3.58	0.02	8.241 (1)	$Li_{1.01}Mn_{1.98}O_4I_{0.02}$	3.54
700	8.213 (1)	$Li_{0.99}Mn_{1.99}O_4I_{0.03}$	3.54	0.04	8.240 (1)	$Li_{1.03}Mn_{1.96}O_4I_{0.04}$	3.58
800	8.229 (2)	$Li_{1.00}Mn_{2.01}O_4I_{0.02}$	3.49	0.07	8.240 (1)	$Li_{1.07}Mn_{1.93}O_4I_{0.10}$	3.64
900	8.231 (2)	$Li_{0.98}Mn_{2.01}O_4$	3.49	0.10	8.239 (1)	$Li_{1.09}Mn_{1.91}O_4I_{0.12}$	3.68

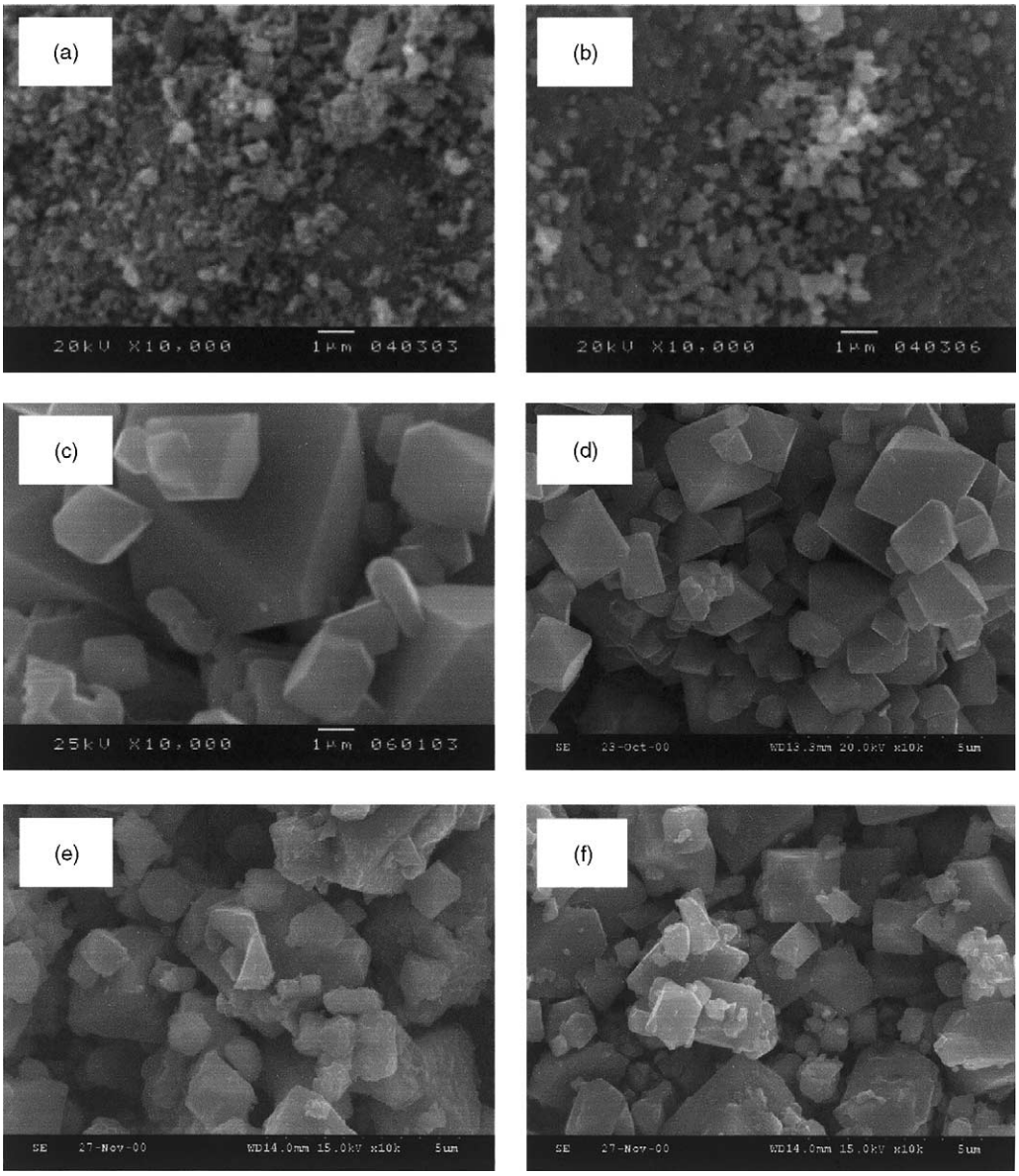

Fig. 2. SEM of ICCD-LMO prepared at: (a) 500 °C, (b) 800 °C, and (c) 900 °C; ICLR-LMO with: (d) $x = 0$, (e) $x = 0.02$, and (f) $x = 0.07$.

At lower temperatures, the crystallites have a spherical shape with small particle sizes about 0.1–0.5 μm. At 900 °C, by contrast, the particles are shaped into well-developed polyhedra of mainly cubic configuration bounded by eight (111) planes as observed in cubic spinel [14]. This morphological difference may be explained by the existence of the iodine species on the surface of ICCD-LMO. During the reaction, crystal growth appears to be inhibited up to 800 °C due to evaporation of the iodine species. At 900 °C, the iodine species are completely evaporated and large crystals develop. For the ICLR-LMO series, the particle size decreases as x increases from 2 μm ($x = 0$) to 0.5 μm ($x = 0.1$). For ICCD-LMO, iodine species at the surface induce local strain due to the large difference in ionic radius between oxide ion and iodine species. Therefore, well-developed $LiMn_2O_4$ particles begin to divide into a smaller ones to release the local strain.

3.4. Electrochemical test

The discharge capacities of ICCD- and ICLR-LMO at a current density of 70 mA g^{-1} are presented in Fig. 3. In contrast to the cycle performance of cation-deficient $Li_{1-\delta}Mn_{2-2\delta}O_4$, it is worthy to note that ICCD-LMO prepared at 800 °C shows the best cycle performance among the ICCD-LMO series. This indicates that a small amount of iodine species enhances cycleability due to surface modification. For ICLR-LMO, the sample with $x = 0.02$ yields the highest discharge capacity and best cycleability, and the initial discharge capacities of ICLR-LMO decrease as x

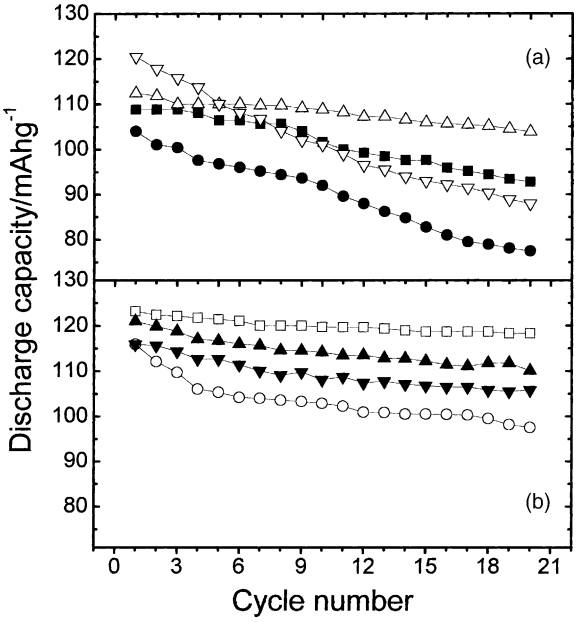

Fig. 3. Evolution of discharge capacities with cycle number. (a) ICCD-LMO prepared at: (●) 500 °C, (■) 700 °C, (△) 800 °C, (▽) 900 °C; (b) ICLR-LMO with: (□) $x = 0.01$, (▲) $x = 0.02$, (▼) $x = 0.04$, (○) $x = 0$.

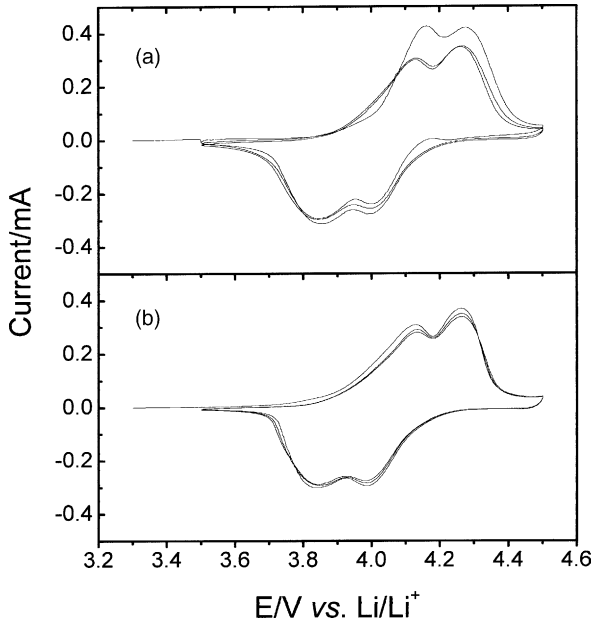

Fig. 5. Cyclic voltammograms of ICLR-LMO powders with: (a) $x = 0$, and (b) $x = 0.02$; scan rate $v = 50\ \mu V\ s^{-1}$.

increases because of the decrease in Mn^{3+} content. Samples with a large amount of iodine species also exhibit poor cycleability. From both ICCD- and ICLR-LMO results, it can be concluded that samples with a small amount of iodine species display good cycleability. This means that the spinel phase is stabilized by the surface modification, but the large size of the iodine species will block the lithium pathway if the iodine content is increased. In this regard, the cycle performance of $LiAl_{0.24}Mn_{1.76}O_{3.98}S_{0.02}$ will degrade if the amount of sulfide ions increases.

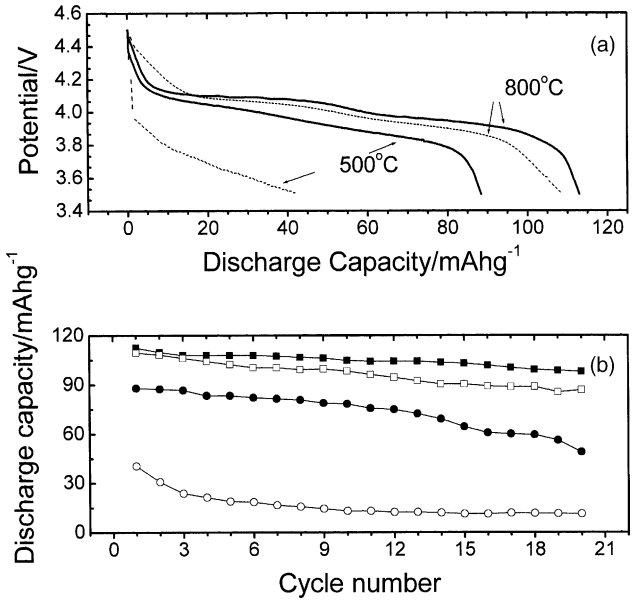

Fig. 4. (a) First charge–discharge voltage profiles of ICCD-LMO prepared at 500 and 800 °C at current density of: (solid lines) 70 mA g^{-1}, (dashed lines) 280 mA g^{-1}; (b) corresponding discharge capacities as a function of cycle number: (■) 800 °C and 70 mA g^{-1}, (□) 800 °C and 280 mA g^{-1}; (●) 500 °C and 70 mA g^{-1}, (○) 500 °C and 280 mA g^{-1}.

The earlier described findings are further confirmed by rate capability and CV. The rate performances of ICCD-LMO prepared at 500 and 800 °C are given in Fig. 4. Obviously, the rate capability of the sample prepared at 800 °C is superior to that of the sample prepared at 500 °C. Cyclic voltammograms of $LiMn_2O_4$ and ICLR-LMO with $x = 0.02$ for the first three cycles are shown in Fig. 5. For two samples, the oxidation and reduction peaks are located around 4.2 and 3.9 V, respectively. For $LiMn_2O_4$, the oxidation and reduction peaks decrease on the second cycle. ICLR-LMO with $x = 0.02$, however, shows very good reversibility for the oxidation–reduction processes.

Thus far, it has been found that ICCD- and ICLR-LMO with a small amount of iodine species show good electrochemical performance. In particular, ICLR-LMO with $x = 0.02$ gave a discharge capacity of 124 mA g^{-1} on the first cycle and 119 mA h g^{-1} on the 20th cycle. Although it has not been possible to identify the form of the iodine species in the samples, the presence of a small amount of iodine enhances the cycleability. Nevertheless, large amounts of iodine species on the surface of the spinel lattice block the pathway for lithium ions and, thus degrade cell performance.

Acknowledgements

We gratefully acknowledge financial support for this work by the Ministry of Education and Human Resources

Development (BK-21) and the Korea Science and Engineering Foundation (KOSEF R01-2001-00045).

References

[1] G.G. Amatucci, A. Blyr, C. Sigala, P. Alfonse, J.M. Tarascon, Solid State Ion. 104 (1997) 13.
[2] A. Yamada, M. Tanaka, K. Tanaka, K. Sekai, J. Power Sources 81 (1999) 73.
[3] R.J. Gummow, A. de Kock, M.M. Thackeray, Solid State Ion. 69 (1994) 59.
[4] G.G. Amatucci, N. Pereira, T. Zheng, I. Plitz, J.M. Tarascon, J. Power Sources 81 (1999) 39.
[5] Y.-K. Sun, Y.-S. Jeon, J. Mater. Chem. 9 (1999) 3147.
[6] J.K. Kim, A. Manthiram, Nature 390 (1997) 265.
[7] X. Yang, W. Tang, H. Kanoh, K. Ooi, J. Mater. Chem. 9 (1999) 2683.
[8] Y.-S. Lee, Y.-K. Sun, K.-S. Nahm, Solid State Ion. 109 (1998) 1285.
[9] M. Yoshio, S. Inoue, M. Hyakatake, G. Piao, H. Nakamura, J. Power Sources 34 (1991) 147.
[10] Y. Gao, J.R. Dahn, J. Electrochem. Soc. 143 (1996) 100.
[11] P. Lucas, C.A. Angell, J. Electrochem. Soc. 147 (2000) 4459.
[12] J. Rodriguez-Carvajal, Fullprof Program, Version 3.2, LLB JRC, January 1997.
[13] J. Kim, A. Manthiram, Electrochem. Solid State Lett. 2 (1999) 55.
[14] T. Takada, H. Enoki, H. Hayakawa, E. Akiba, J. Solid State Chem. 139 (1998) 290.